Programming and control for human robot interaction

Atussa Koushan - 03713848

June 2019

Contents

2 Theory

2.2 Joints control

2.2.1 PD controller

The law of the PD controller for reaching the desired joint position q_d when $\dot{q_d} = 0$ is

$$\tau = K_p(\mathbf{q_d} - \mathbf{q}) - K_d\dot{\mathbf{q}} \tag{1}$$

2.2.2 Controlled system dynamics

The equation of the dynamics of the PD controlled system is as follows.

$$\mathbf{M}(\mathbf{q})\ddot{\mathbf{q}} + \mathbf{C}(\mathbf{q}, \dot{\mathbf{q}})\dot{\mathbf{q}} + \mathbf{g}(\mathbf{q}) = \mathbf{K_p}(\mathbf{q_d} - \mathbf{q}) - \mathbf{K_d}\dot{\mathbf{q}} \tag{2}$$

2.2.3 Damping matrix K_d

Neglecting the centrifugal and Coriolis forces and assuming a quasi-stationary variation, the controlled dynamics can be written

$$\mathbf{M}(\mathbf{q})\ddot{\tilde{\mathbf{q}}} + \mathbf{K_d}\dot{\tilde{\mathbf{q}}} + \mathbf{K_p}\tilde{\mathbf{q}} = \mathbf{0} \tag{3}$$

where $\tilde{\mathbf{q}} = \mathbf{q_d} - \mathbf{q}$.
We now derive the damping matrix $\mathbf{K_d}$ for achieving a given damping factor ζ of the system with a constant stiffness matrix $\mathbf{K_p}$.

$$\ddot{\mathbf{q}} + \mathbf{2}\zeta\omega_\mathbf{0}\dot{\mathbf{q}} + \omega_\mathbf{0}^\mathbf{2}\mathbf{q} = \mathbf{ku} \tag{4}$$

Comparing (3) and (4) we get

$$\omega_\mathbf{0}^\mathbf{2} = \mathbf{M^{-1}}(\mathbf{q_0})\mathbf{K_p} \Longrightarrow \omega_\mathbf{0} = \sqrt{\mathbf{M^{-1}}(\mathbf{q_0})\mathbf{K_p}} \tag{5}$$

$$2\zeta\omega_\mathbf{0} = \mathbf{M}(\mathbf{q_0})^{-\mathbf{1}}\mathbf{K_d} \Longrightarrow \mathbf{K_d} = 2\zeta\sqrt{\mathbf{M}(\mathbf{q_0})\mathbf{K_p}} \tag{6}$$

2.4 Translational Cartesian Impedance control

2.4.1 Cartesian forces and torques

$$\dot{\mathbf{x}} = \mathbf{J}(\mathbf{q})\dot{\mathbf{q}} \tag{7}$$

$$power = \dot{\mathbf{x}}^\mathbf{T}\mathbf{F} = \dot{\mathbf{q}}^\mathbf{T}\tau \tag{8}$$

From inserting (7) in (8) we get the mapping between joint torques and Cartesian forces:

$$\tau = \mathbf{J}^\mathbf{T}(\mathbf{q})\mathbf{F} \tag{9a}$$

$$\mathbf{F} = (\mathbf{J}^\mathbf{T}(\mathbf{q}))^{-\mathbf{1}}\tau \tag{9b}$$

2.4.2 Spring force $\mathbf{F}_K$

Considering a translational error $\tilde{\mathbf{x}} = \mathbf{x} - \mathbf{x_d}$ and a constant, positive definite symmetric stiffness matrix $\mathbf{K}_t \in \mathbb{R}^2$, the law of a spring force $\mathbf{F}_K$ between the TCP of the manipulator and the desired point can be written

$$\mathbf{F}_K = \mathbf{K}_t \tilde{\mathbf{x}} \tag{10}$$

2.4.3 Damping force $\mathbf{F}_D$

The planar Cartesian force resulting from a viscous damper with the constant symmetric damping matrix $\mathbf{D}_t \in \mathbb{R}^2$ is

$$\mathbf{F}_D = -\mathbf{D}_t \dot{\mathbf{x}} \tag{11}$$

2.4.4 Cartesian impedance controller

The Cartesian impedance control law below is derived from (10), (11) and (9a).

$$\tau_\mathbf{i} = \mathbf{J^T}(\mathbf{q})(\mathbf{F_K} + \mathbf{F_D}) = \mathbf{J^T}(\mathbf{q})(\mathbf{K_t}\tilde{\mathbf{x}} - \mathbf{D_t}\dot{\mathbf{x}}) \tag{12}$$

2.5 Nullspace optimizations

In this section a control law for the nullspace motion will be derived. Adding the nullspace torque $\tau_\mathbf{n}$ and impedance controller torque $\tau_\mathbf{i}$ together we get the complete impedance controller (13).

$$\tau = \tau_\mathbf{i} + \tau_\mathbf{n} \tag{13}$$

2.5.1 Nullspace control law $\tau_\mathbf{n}$

The nullspace control law is

$$\tau_\mathbf{n1} = (\mathbf{I} - \mathbf{J^T}\mathbf{J^{+T}})\tau_\mathbf{0}, \tag{14}$$

where $(\mathbf{I} - \mathbf{J^T}\mathbf{J^{+T}})$ is the orthogonal projection matrix onto the nullspace.

As we disregard the rotation, the last row of the Jacobian is removed. Because of this $\mathbf{J}$ is no longer quadratic and we have to use the pseudo inverse instead of the inverse. The projection matrix is thus zero on all elements that could interfere with the TCP torque.

2.5.2 Pseudo inverse

The expression of the pseudo inverse is

$$\mathbf{J^+} = \mathbf{J^T}(\mathbf{J}\mathbf{J^T})^{-\mathbf{1}}. \tag{15}$$

It holds the following property

$$\mathbf{J}\mathbf{J^+} = \mathbf{J}\mathbf{J^T}(\mathbf{J}\mathbf{J^T})^{-\mathbf{1}} = \mathbf{J}\mathbf{J^T}\mathbf{J^{-T}}\mathbf{J^{-1}} = \mathbf{I}. \tag{16}$$

2.5.3 Damping nullspace torque τ_0

The joint velocity is used to obtain a damping motion.

$$\tau_{\mathbf{0}} = \mathbf{D}\dot{\mathbf{q}} \tag{17}$$

2.5.4 Singular configurations

A singularity is a manipulator configuration in which at least one degree of freedom is lost (becomes uncontrollable) through parallel axes (links). This can be observed by analyzing the Jacobian and the relationship $\tau = \mathbf{J^T F}$. If a force is acting in a singular direction the corresponding torques will be zero since the Jacobian is singular in singular configurations.

2.5.5 Quadratic potential function

An index of manipulability for the manipulator is given by

$$m_{kin}(\mathbf{q}) = \sqrt{l_1^2 l_2^2 \sin^2 q_2} \tag{18}$$

As this measure gives the distance to the singularity, we can base the quadratic potential function (19) on it to control the gain of the singularity avoidance.

$$U(m_{kin}) = \frac{1}{2} m_{kin}^T k_s m_{kin} \tag{19}$$

2.5.6 Control torque for singularity avoidance

A control torque that implements the singularity avoidance by means of the potential function in (19) is given in (20).

$$\tau_{\mathbf{n2}} = \begin{cases} -k_s m_{kin}(m_{kin} - \alpha)\cot q_2, & \text{if } m_{kin} \leq \alpha \\ 0, & \text{otherwise} \end{cases} \tag{20}$$

Here the threshold α implements the piecewise definition of the torque to testrict the potential to the vicinity of the singularity.

2.5.7 Complete control law

By combining (12), (14) and (20) the complete control law becomes

$$\begin{aligned} \tau &= \tau_{\mathbf{i}} + \tau_{\mathbf{n1}} + \tau_{\mathbf{n2}} \\ &= \mathbf{J^T}(\mathbf{q})(\mathbf{K_t}\tilde{\mathbf{x}} - \mathbf{D_t}\dot{\mathbf{x}}) + (\mathbf{I} - \mathbf{J^T J^{+T}})(\tau_{\mathbf{0}} - k_s m_{kin}(m_{kin} - \alpha)\cot q_2) \end{aligned} \tag{21}$$

2.7 Collision detection

2.7.1 External torque estimation

A scheme for estimating only the external torques (i.e. not including the friction forces) is shown in figure 1.

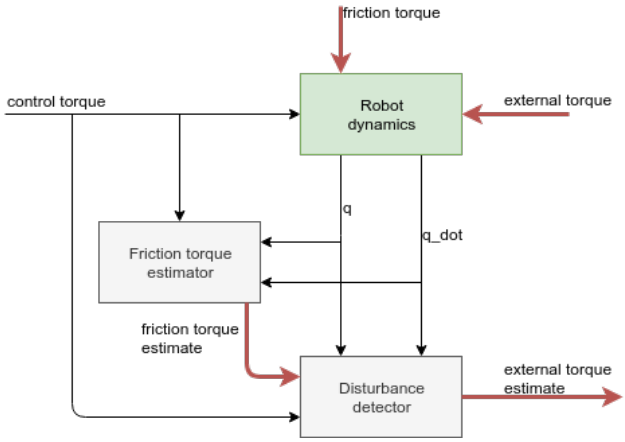

Figure 1: Scheme for estimating only the external torques

2.7.2 Effective torque τ_e deduction

The disadvantage of deducing the effective torque from measurements is that measurements, and in particular acceleration signals, tend to be noisy.

Deducing it from the desired trajectory might also lead to deviations from the true value as the controller dynamics aren't considered and the manipulator itself might not be in the desired configuration at all times.

2.7.3 Variation of momentum

The variation of the momentum $\dot{\mathbf{p}}$ is derived from differentiating the momentum in (23) and using the standard robot property $\dot{M} = C + C^T$ as well as the manipulator dynamics in (22).

$$\mathbf{M}(\mathbf{q})\ddot{\mathbf{q}} + \mathbf{C}(\mathbf{q}, \dot{\mathbf{q}})\dot{\mathbf{q}} + \mathbf{g}(\mathbf{q}) = \tau \tag{22}$$

$$\mathbf{p} = \mathbf{M}(\mathbf{q})\dot{\mathbf{q}} \tag{23}$$

$$\begin{aligned} \dot{\mathbf{p}} &= \mathbf{M}(\mathbf{q})\ddot{\mathbf{q}} + \dot{\mathbf{M}}(\mathbf{q})\dot{\mathbf{q}} \\ &= \mathbf{M}(\mathbf{q})\ddot{\mathbf{q}} + \mathbf{C}(\mathbf{q}, \dot{\mathbf{q}})\dot{\mathbf{q}} + \mathbf{C^T}(\mathbf{q}, \dot{\mathbf{q}})\dot{\mathbf{q}} \\ &= \tau + \mathbf{C^T}(\mathbf{q}, \dot{\mathbf{q}})\dot{\mathbf{q}} - \mathbf{g}(\mathbf{q}) \end{aligned} \tag{24}$$

2.7.4 Collision estimator

A scheme of the collision (external torque) estimator based on the impulse is shown if figure 2.

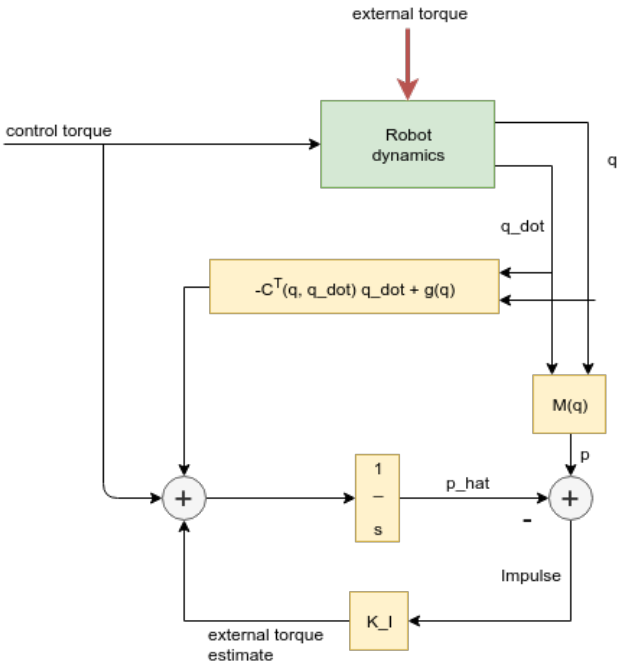

Figure 2: Scheme of external torque estimation

2.7.5 Estimator dynamics

$$\hat{\tau}_K = K_I(p - \hat{p}) \tag{25}$$

$$\begin{aligned} \dot{\hat{\tau}}_K &= K_I(\dot{p} - \dot{\hat{p}}) \\ &= K_I[\tau + \tau_K + C^T(q,\dot{q})\dot{q} - g(q) - (\tau + \hat{\tau}_K + C^T(q,\dot{q})\dot{q} - g(q))] \\ &= K_I(\tau_K - \hat{\tau}_K) \end{aligned} \tag{26}$$

$$\dot{\hat{\tau}}_K + K_I\hat{\tau_K} = K_I\tau_K \tag{27}$$

2.7.6 Collision reaction strategies

In case of collision the following listed reaction strategies can be adopted.

- Stop the robot.
- Switch to gravity compensation.
- Fast movement in force direction (reflex reaction).
- Slowing down or reversing the trajectory by modifying the interpolate point in position control mode.

3 Simulation

3.1 Kinematics and dynamics

Figure 3 shows the simulated response of the joint angles when initialized at $\mathbf{q}_i = [-60°, -30°, 20°]$. This initial configuration is used in all of the following tasks as well. As expected the manipulator falls down and ends up hanging downwards as the only external force having an impact on it's position is the gravity. Since the initial configuration is slightly different from the straight downwards pose and we start off with some potential energy, there are some oscillations around the equilibrium before it settles.

3.2 Joints control

Gravity compensation is now added to the manipulator. As expected it is observed that the manipulator simply stays in its initial configuration. The response is shown in figure 4.

A PD controller and friction with coefficient 1 is introduced to the system. If we deactivate the gravity compensation the controller is not able to bring the manipulator to the desired position, therefore it is left on for the rest of the simulation.

The stiffness and damping matrices $\mathbf{K_p}$ and $\mathbf{K_d}$ are tuned to achieve a fast and well damped response. Three different combinations of the values of $\mathbf{K_p}$ and $\mathbf{K_d}$ are presented in the plots below. Note that $\mathbf{K_p}$ and $\mathbf{K_d}$ are diagonal matrices with constant values on the diagonal. The desired joint configuration is set to $\mathbf{0}$.

From figure 5 it is clear that a large stiffness and low damping results in an underdamped system with oscillations around the desired configuration. Increasing the damping and decreasing the stiffness will on the other hand lead to an overdamped response as seen in figure 6. The best control parameters to provide a critically damped response were by trial and error found to be

$$\mathbf{K_p} = \begin{bmatrix} 18 & 0 & 0 \\ 0 & 18 & 0 \\ 0 & 0 & 18 \end{bmatrix}, \mathbf{K_d} = \begin{bmatrix} 12 & 0 & 0 \\ 0 & 12 & 0 \\ 0 & 0 & 12 \end{bmatrix} \tag{28}$$

The damping matrix is now calculated with the method of the square root matrices as shown in section 2.2.3. $\mathbf{K_p}$ is kept as in (28) while the damping factor is changed to obtain different responses.

Overdamped case:

$$\zeta = 3 \Longrightarrow \mathbf{K_d} = \begin{bmatrix} 46.2 & 19.8 & 5.4 \\ 19.8 & 19.1 & 5.2 \\ 5.4 & 5.2 & 6.6 \end{bmatrix} \tag{29}$$

Critically damped case:

$$\zeta = 1 \Longrightarrow \mathbf{K_d} = \begin{bmatrix} 15.4 & 6.6 & 1.8 \\ 6.6 & 6.4 & 1.7 \\ 1.8 & 1.7 & 2.2 \end{bmatrix} \tag{30}$$

Underdamped case:

$$\zeta = 0.3 \Longrightarrow \mathbf{K_d} = \begin{bmatrix} 4.6 & 2.0 & 0.54 \\ 2.0 & 1.9 & 0.52 \\ 0.54 & 0.52 & 0.66 \end{bmatrix} \tag{31}$$

3.4 Translational Cartesian Impedance control

A translational Cartesian controller is now implemented using the control law from 2.4.4. The friction is still left on. It is observed that trying to command the position to $[x, y] = [0, 1.5]$, which is outside the workspace of the manipulator, will move the manipulator to $[x, y] = [0, 1]$. This is because the length of the manipulator when it is in its completely stretched out configuration is 1. This configuration is also called a singular position where the Jacobian becomes zero and we lose a degree of freedom.

Some diagonal matrices are tested for the spring- and damping matrices. Since we only take the x- and y position into consideration the last diagonal element is set to zero in all of tested matrices. Three characteristic combinations are shown in figures 11, 12 and 13. The desired configuration is set to be $[x, y] = [0.5, 0.5]$ in all cases.

In the first example (figure 11) the spring constant is a lot bigger than the damping. This results in the manipulator oscillating a lot around the desired position.

In the second example (figure 12) we get the opposite problem as the damping matrix is dominant and it takes a long time for the manipulator to get to the desired position.

Lastly, the result of an optimal combination of K_t and D_t (see (32)) is shown in figure 13. The desired configuration is achieved with a fast and damped motion with a small overshoot.

$$\mathbf{K_t} = \begin{bmatrix} 14 & 0 & 0 \\ 0 & 14 & 0 \\ 0 & 0 & 0 \end{bmatrix}, \mathbf{D_t} = \begin{bmatrix} 13 & 0 & 0 \\ 0 & 13 & 0 \\ 0 & 0 & 0 \end{bmatrix} \tag{32}$$

3.5 Nullspace optimization

For this task the friction is disabled, and

$$\mathbf{K_t} = \begin{bmatrix} 16 & 0 & 0 \\ 0 & 16 & 0 \\ 0 & 0 & 0 \end{bmatrix}, \mathbf{D_t} = \begin{bmatrix} 25 & 0 & 0 \\ 0 & 25 & 0 \\ 0 & 0 & 0 \end{bmatrix}. \tag{33}$$

The nullspace controller from section 2.5 is implemented with nullspace damping coefficient $\mathbf{D} = -6$. The desired Cartesian position is set to be $[x, y] = [0.3, 0]$. As this is the length of one link, a natural configuration for the robot to reach this position is simply moving in such a manner that the first two links overlap (they end up parallel to each other). Figure 14a shows that the desired configuration is reached, however, since the first links overlap, the robot is in a singularity. This can be seen from figure 14b which shows the distance to a singularity which is practically 0.

Introducing the nullspace singularity avoidance from section 2.5 to the controller with a threshold $\alpha = 0.08$ and $k_s = 10000$ enables the robot to avoid this singularity. From figure 15b it is seen that the manipulator starts moving away from the singularity when m_{kin} goes below 0.08. With the singularity avoidance it is also able to reach its desired position in a fast manner (figure 15a).

3.7 Collision detection

The external torque estimator from figure 2 is implemented. For this task the friction is included and the control parameters are as found in section 3.4. From figure 16 it can be seen that the estimator is correctly "detecting" a collision at 1 second.

A source of noise is now added to the joint angles and velocities $\mathbf{q}, \dot{\mathbf{q}}$. The behaviour of the estimator varies with the choice of K_I. From figures 17 to 19 it can be observed that a higher gain results in a faster, but more noisy, response. The best compromise seems to be $K_I = 10$.

A Figures

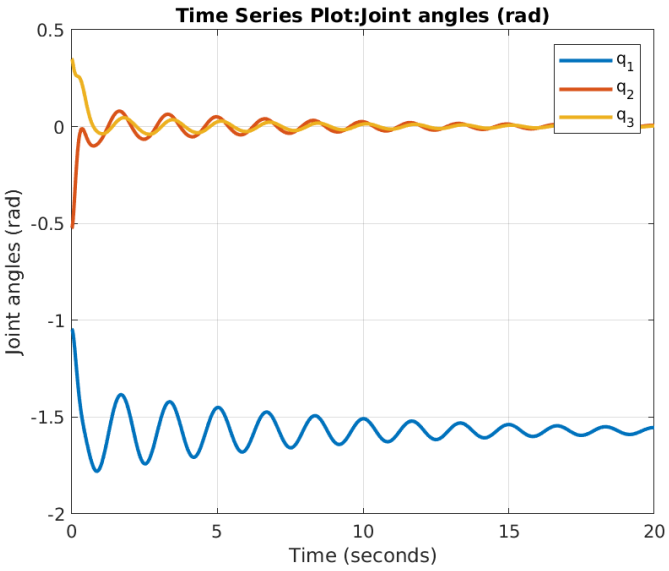

Figure 3: Joint angles response without controller

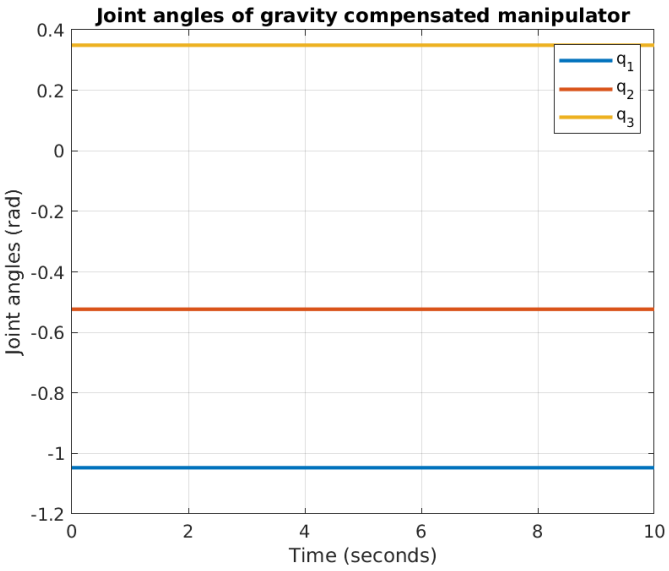

Figure 4: Joint angles response with gravity compensation

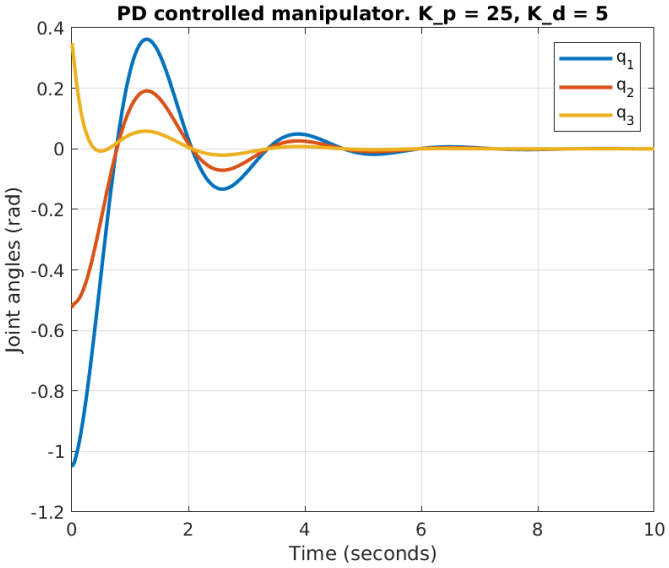

(a) Joint angles

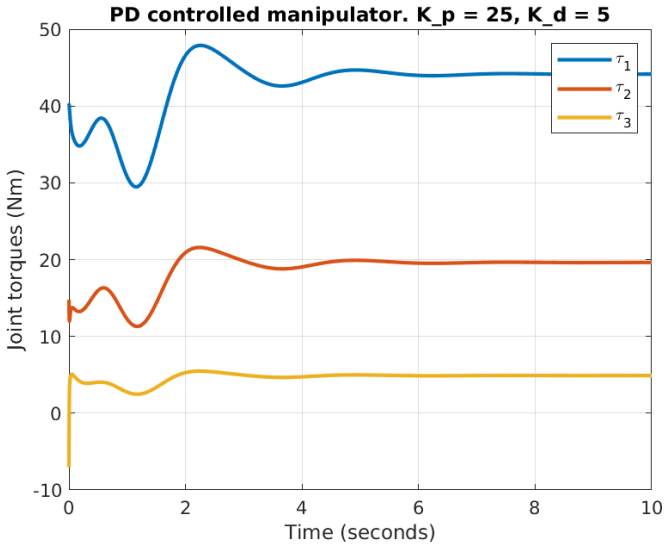

(b) Joint torques

Figure 5: PD controlled manipulator with $\mathbf{K_p} = 25$ and $\mathbf{K_d} = 5$

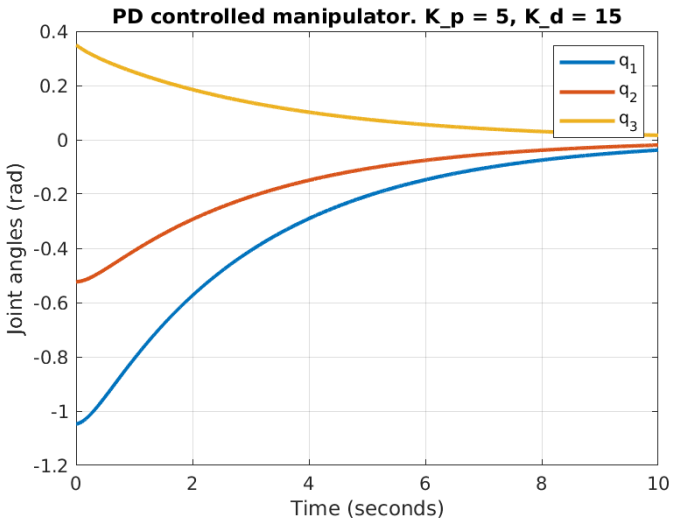

(a) Joint angles

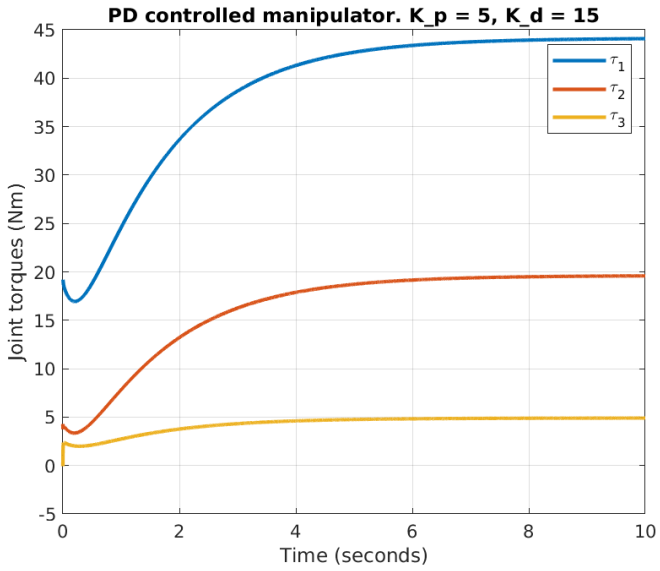

(b) Joint torques

Figure 6: PD controlled manipulator with $\mathbf{K_p} = 5$ and $\mathbf{K_d} = 15$

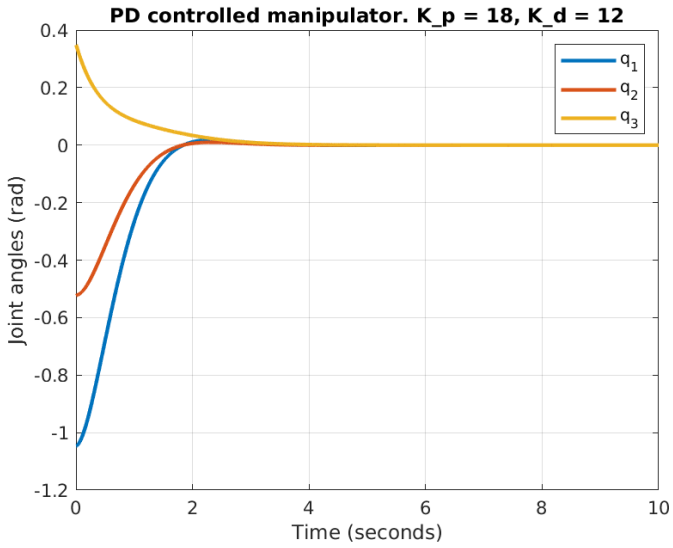

(a) Joint angles

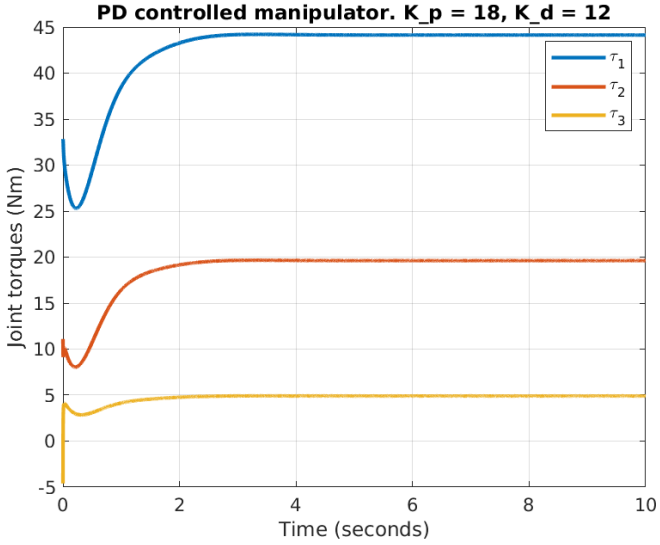

(b) Joint torques

Figure 7: PD controlled manipulator with $\mathbf{K_p} = 18$ and $\mathbf{K_d} = 12$

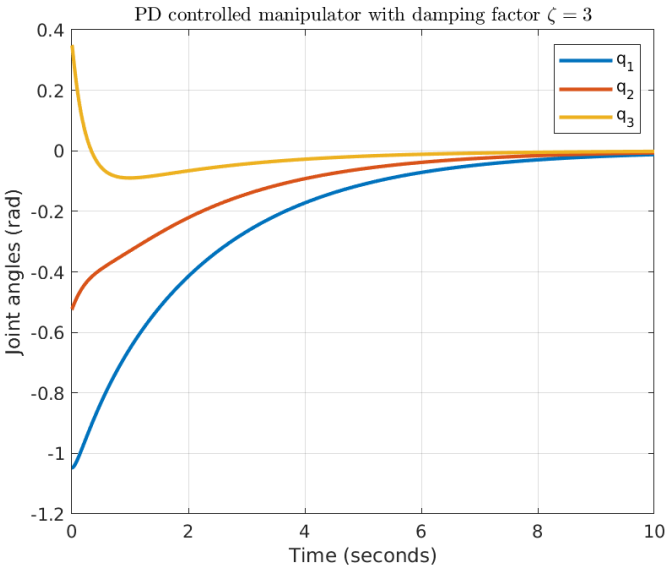

(a) Joint angles

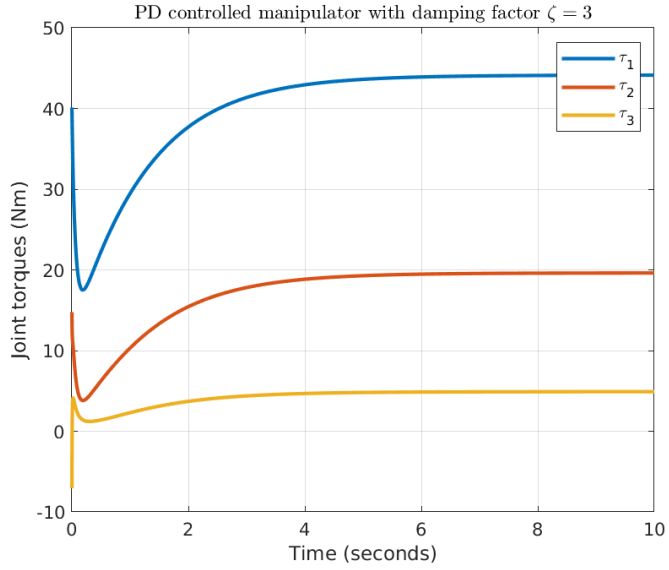

(b) Joint torques

Figure 8: PD controlled manipulator with damping factor $\zeta = 3$

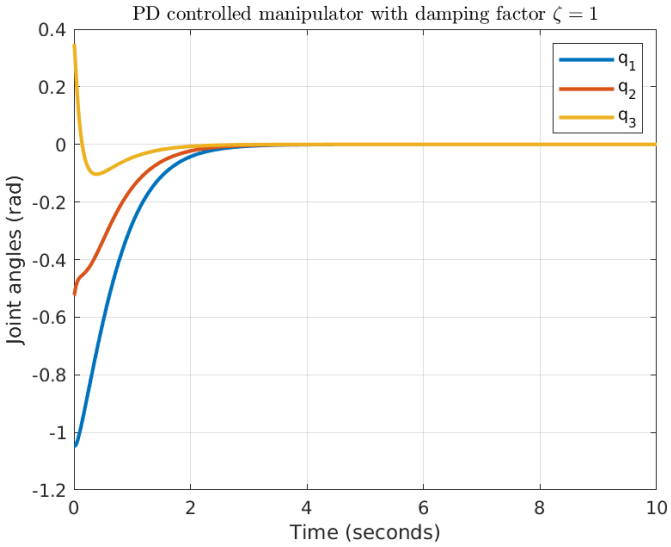

(a) Joint angles

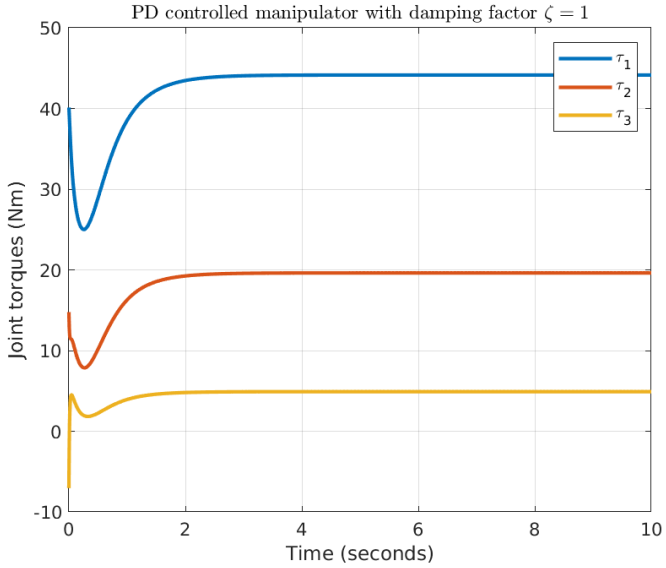

(b) Joint torques

Figure 9: PD controlled manipulator with damping factor $\zeta = 1$

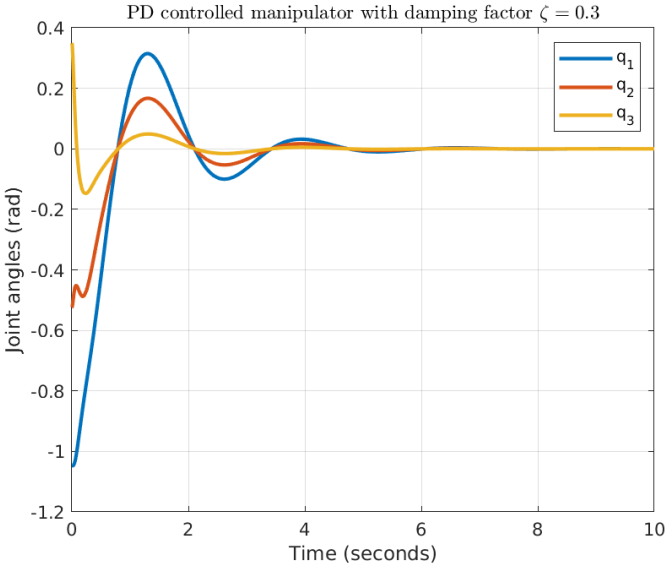

(a) Joint angles

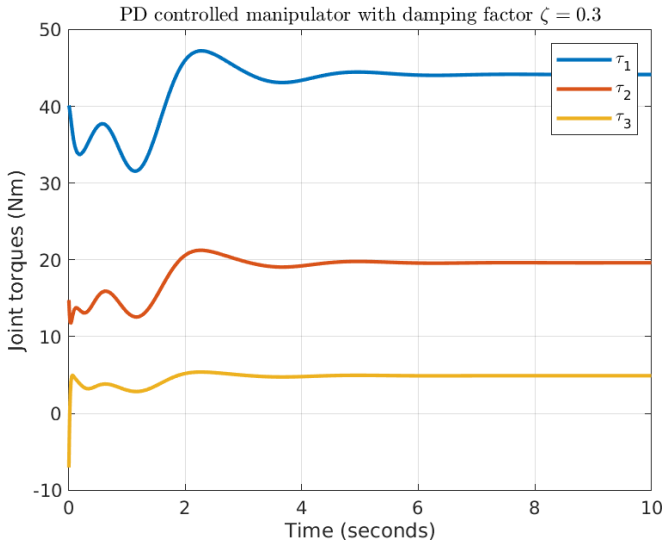

(b) Joint torques

Figure 10: PD controlled manipulator with damping factor $\zeta = 0.3$

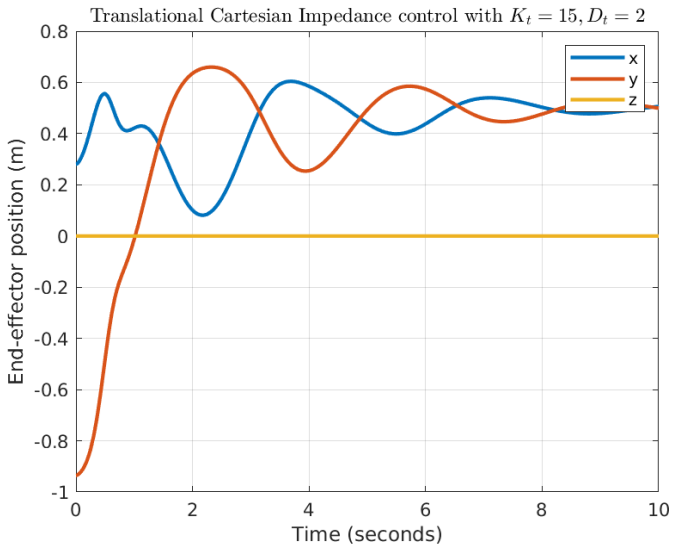

Figure 11: Translational Cartesian Impedance control with $K_t = 15, D_t = 2$

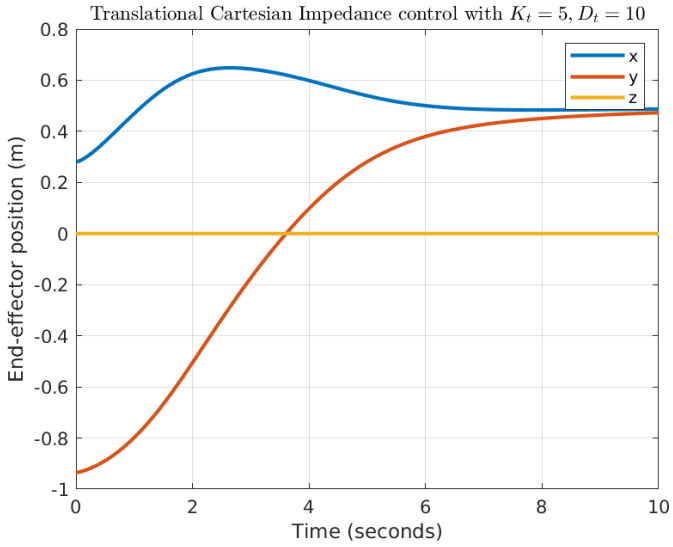

Figure 12: Translational Cartesian Impedance control with $K_t = 5, D_t = 10$

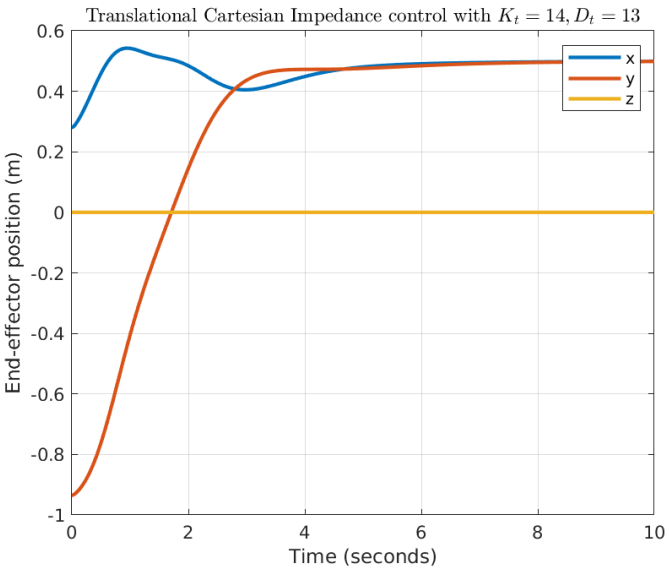

Figure 13: Translational Cartesian Impedance control with $K_t = 14, D_t = 13$

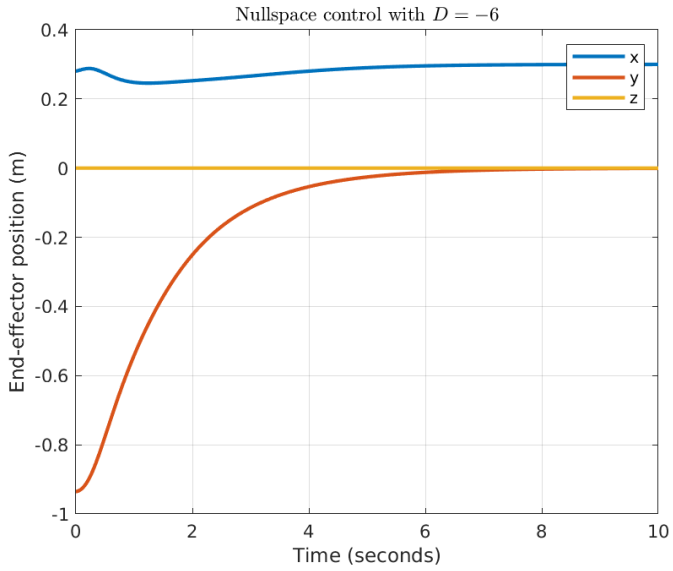

(a) Cartesian position

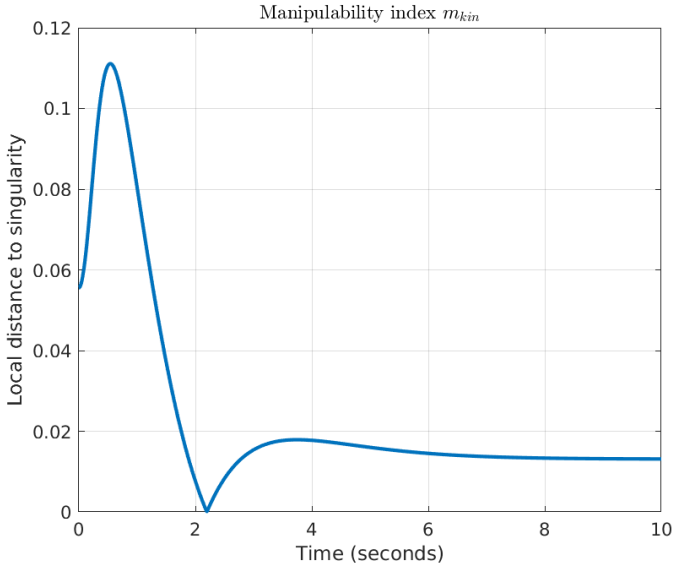

(b) Manipulability index

Figure 14: Nullspace control without singularity avoidance

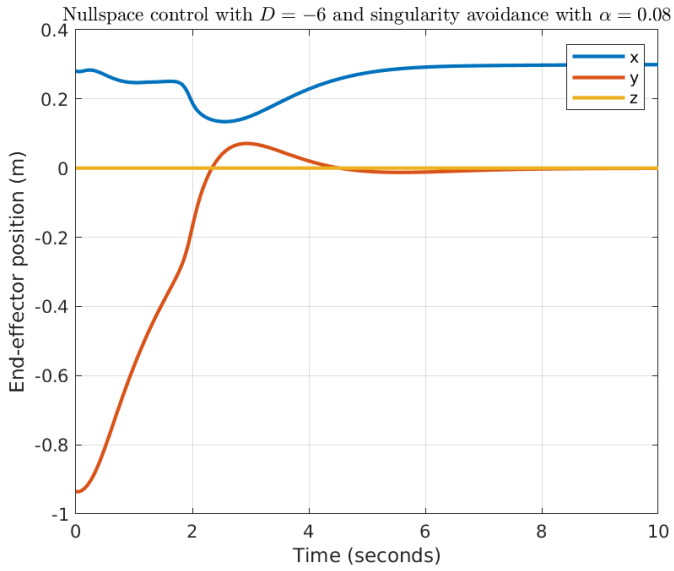

(a) Cartesian position

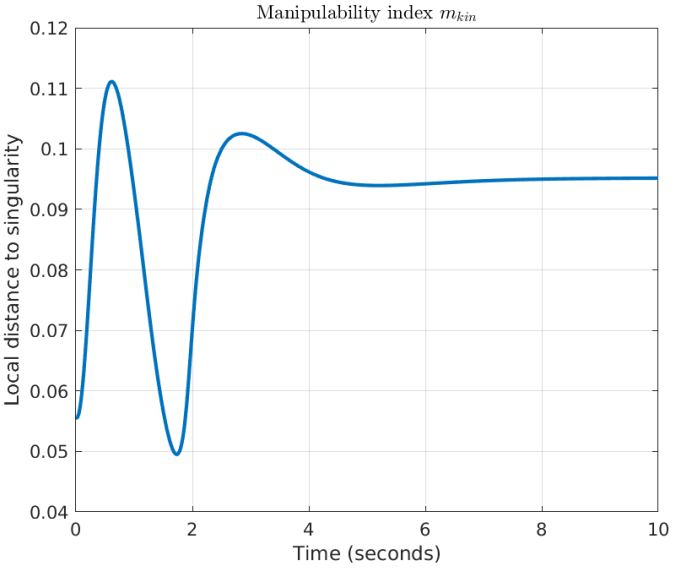

(b) Manipulability index

Figure 15: Nullspace control with singularity avoidance $\alpha = 0.08$

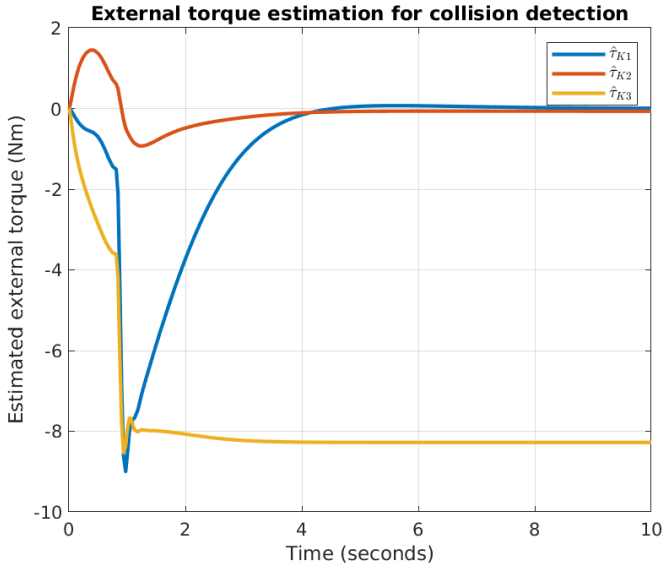

(a) External torque

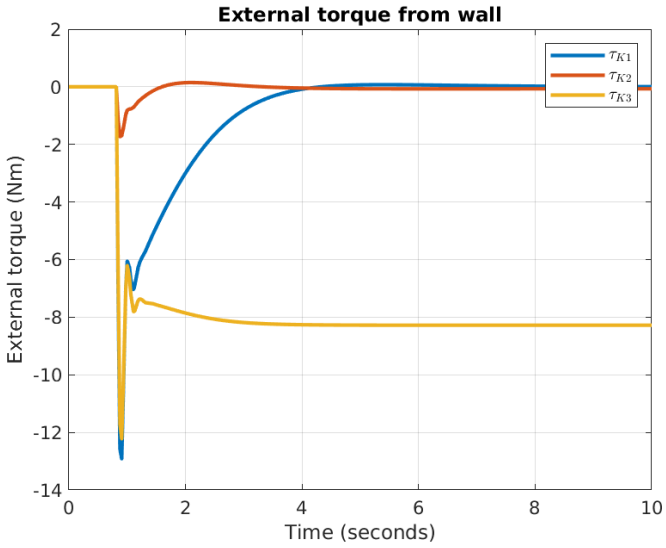

(b) Estimated external torque

Figure 16: Collision detection

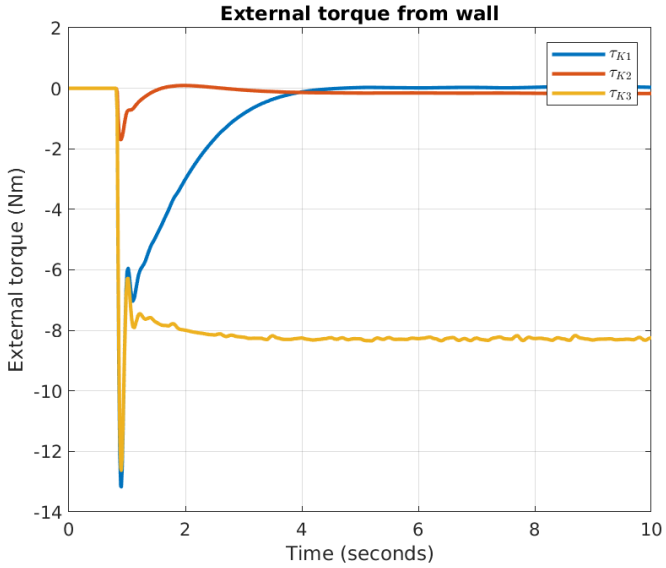

(a) External torque

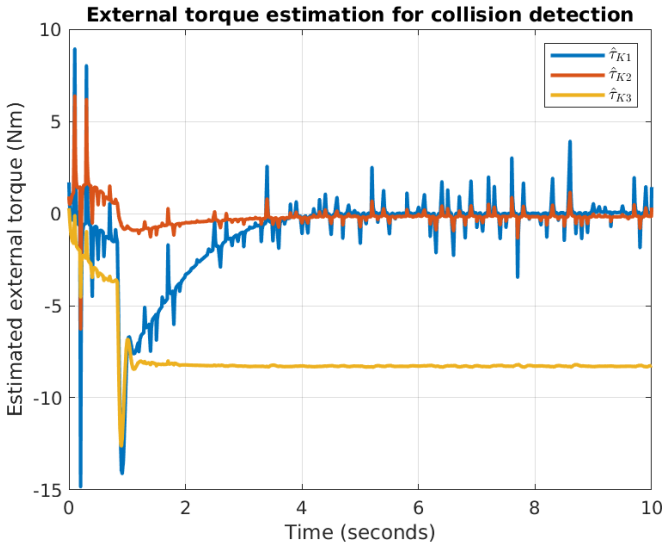

(b) Estimated external torque

Figure 17: Collision detection with $K_I = 100$

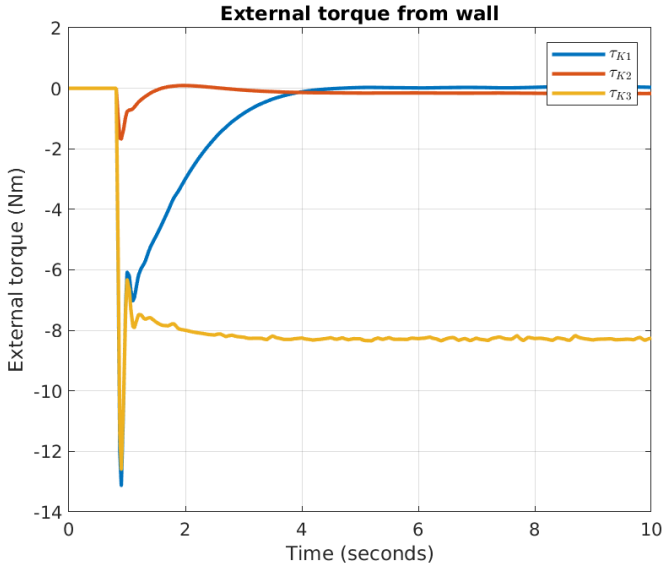

(a) External torque

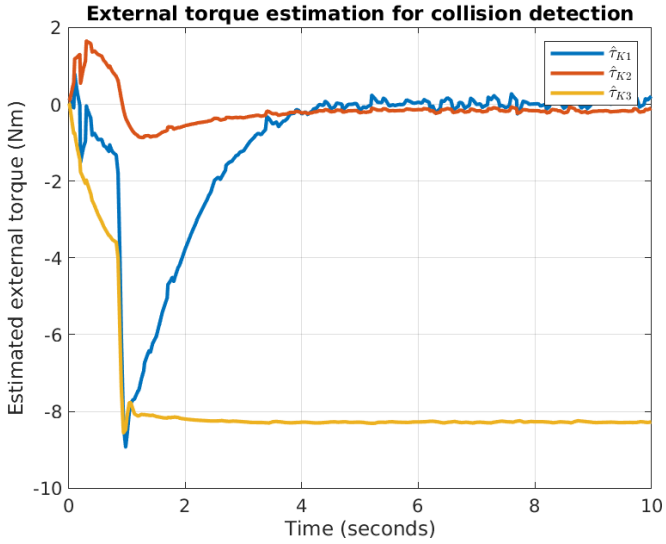

(b) Estimated external torque

Figure 18: Collision detection with $K_I = 10$

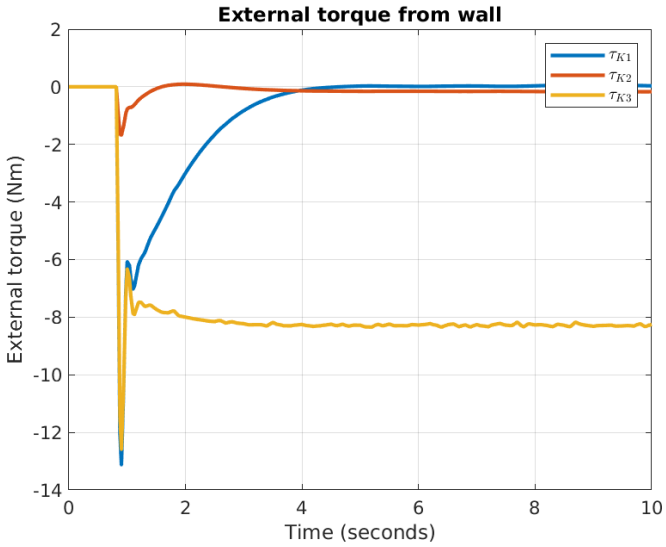

(a) External torque

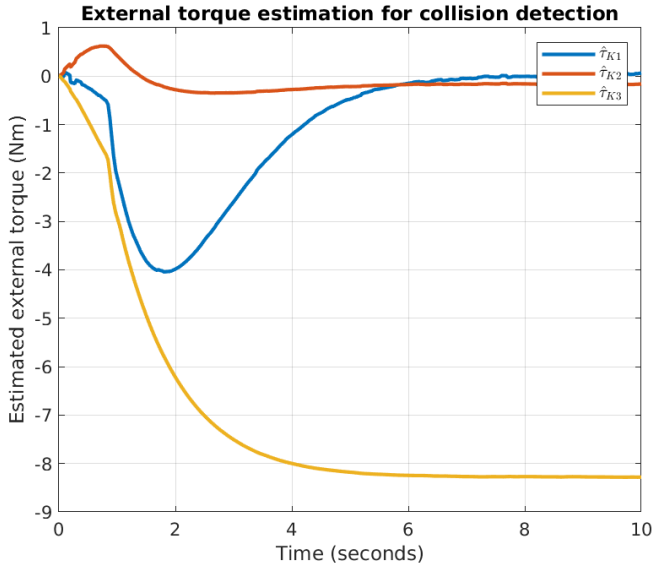

(b) Estimated external torque

Figure 19: Collision detection with $K_I = 1$